A full-duplex optical access system with hybrid 64/16/4QAM-OFDM downlink*

HE Chao (贺超)**, **TAN Ze-fu** (谭泽富), **SHAO Yu-feng** (邵宇丰), **CAI Li** (蔡黎), **PU He-sheng** (蒲鹤升), **ZHU Yun-le** (朱云乐), **HUANG Si-si** (黄思斯), and **LIU Yu** (刘毓)

Key Laboratory of Signal and Information Processing, College of Electronic & Information Engineering, Chongqing Three Gorges University, Wanzhou 404100, China

(Received 10 August 2016)

A full-duplex optical passive access scheme is proposed and verified by simulation, in which hybrid 64/16/4-quadrature amplitude modulation (64/16/4QAM) orthogonal frequency division multiplexing (OFDM) optical signal is for downstream transmission and non-return-to-zero (NRZ) optical signal is for upstream transmission. In view of the transmitting and receiving process for downlink optical signal, in-phase/quadrature-phase (I/Q) modulation based on Mach-Zehnder modulator (MZM) and homodyne coherent detection technology are employed, respectively. The simulation results show that the bit error ratio (*BER*) less than hardware decision forward error correction (HD-FEC) threshold is successfully obtained over transmission path with 20-km-long standard single mode fiber (SSMF) for hybrid downlink modulation OFDM optical signal. In addition, by dividing the system bandwidth into several sub-channels consisting of some continuous subcarriers, it is convenient for users to select different channels depending on requirements of communication.

Document code: A **Article ID:** 1673-1905(2016)05-0361-5

DOI 10.1007/s11801-016-6176-1

Recently, different bandwidth requirements for high speed data services of different end users have attracted more and more attention in passive optical network (PON) based on orthogonal frequency division multiplexing (OFDM) as a multi-carrier modulation (MCM) technology due to inherent various advantages of high spectral efficiency (SE), powerful digital signal processing (DSP), strong tolerance to both chromatic dispersion and polarization mode dispersion (PMD)[1-5]. However, OFDM signal also faces with a large number of disadvantages, such as high peak-to-average power ratio (*PAPR*) and more sensitivity to frequency offset and phase noise[2]. Therefore, it is worthwhile pointing out that both training symbols-based channel estimation and pilot symbols-based carrier phase estimation have been broadly studied in OFDM demodulation to compensate for chromatically dispersion (CD), fiber nonlinearities, PMD and polarization dependent loss (PDL) and to remove phase shift over time, respectively. Compared with the direct detection optical OFDM PON (DDO-OFDM-PON) for short reach applications, the coherent detection optical OFDM PON (CO-OFDM-PON) for long haul applications further takes into account better sensitivity, more efficient channel equalization, stronger dispersion tolerance and higher SE at the cost of additional optical and electrical components and computational complexity in the form of coherent detection[3-5]. Anyway, the traditional time and wavelength division multiplexed based PONs (TWDM-PONs) and ultra-dense wavelength division multiplexing-based PONs (UDWDM-PONs) have been widely deployed in all over the world[6-10]. Moreover, the PON system transmitted over the optical distribution networks (ODNs) based on OFDM signal has generally been considered as a promising candidate technology for the next generation broadband optical access networks (OANs). In addition, more and more multilevel quadrature amplitude modulation (M-QAM) has been considered as a promising and likely modulation technology for OFDM-based PON transmission architecture over both the downstream and the upstream link to strongly overcome redundancy cost, further improve transmission capacity, easily enhance SE and largely relax bandwidth requirement of electronic components. In the past decades, several critical technologies for OFDM-PON system utilizing M-QAM format have been investigated in order to promote SE and maintain system security in the proposed architectures[11-14]. Some researchers have reported that the encryption of 10 Gbit/s 16 quadrature amplitude modulation (16QAM) OFDM and 12.5 Gbit/s 32QAM OFDM signals based on chaos

* This work has been supported by the National Natural Science Foundation of China (No.61107064), the Chongqing University Innovation Team Founding (No.KJTD201320), and the Chongqing Science and Technology Commission Foundation (No.cstc2016jcyjA1233).

** E-mail: hechaoctgu@163.com

coding enabled by a pair of key sequences has been successfully implemented over 30-km-long standard single mode fiber (SSMF) in the security improved OFDM-PON[11]. Hu et al[12] have experimentally demonstrated the transmission of 8.9 Gbit/s 16QAM OFDM signals based on chaotic partial transmit sequence (CPTS) for physical layer security over 20-km-long SSMF. Lefebvre K et al[13] showed the experimental demonstration of 64QAM and QPSK OFDM uplink and OOK downlink transmission in long reach WDM-PON systems based on reflective semiconductor optical amplifier (RSOA) and achieved *BER* below forward error correction (FEC) threshold. The broadcast of chaos in-phase/quadrature-phase (I/Q) encryption optimal frame transmission (OFT) technique-based 11.32 Gbit/s 16QAM OFDM signal over 25-km-long SSMF had been successfully proposed in Ref.[14]. Real-time reconfigurable 4/16/64 QAM OFDM signal transmission in an X-band radio-over-fiber (RoF) system has been demonstrated by Chen M et al[15] for the first time, where the *BER* less than the hardware decision FEC (HD-FEC) threshold of 3.8×10^{-3} can be achieved after both 1.5-m-long wireless delivery and 2.26-km-long SSMF transmission.

In this paper, a 40 Gbit/s optical access system with hybrid 64/16/4QAM-OFDM downstream link for improved SE and lower complexity enabled by advanced DSP technology is demonstrated in simulation. As we know, this is the first simulation investigation using hybrid 64/16/4QAM OFDM signal for downlink and non-return-to-zero (NRZ) optical signal for uplink transmission based on PON system. We find that high-level QAM is more sensitive to the received optical power (*ROP*) in this full-duplex PON system.

Commonly, the architecture of the next-generation optical access network is illustrated in Fig.1, which contains the only optical line terminal (OLT) deployed in the central station (CS), a few of optical network units or optical network terminals (ONUs/ONTs) installed in the base station (BS), the optical distribution node (ODN) with SSMF, and the passive splitter/combiner (PSC) between the OLT and the ONUs. A great deal of superiorities, such as flexible dynamic bandwidth allocation (DBA), high SE, convergence access based on combination of wired and wireless and excellent resistance chromatic dispersion, make OFDM-PON become a promising technology for the next generation optical access systems.

Fig.2 gives the subcarrier allocation of the proposed OFDM based on hybrid inverse fast Fourier transform and fast Fourier transform (IFFT/FFT), in which 4/16/64QAM is simultaneously modulated and demodulated over 128 sub-carriers, namely, the 5—44 sub-carriers, the 45—84 sub-carriers, and the 85—124 sub-carriers are ideally used for 4QAM, 16QAM and 64QAM, respectively. For the downlink transmitter, serial/parallel (S/P), IFFT, cyclic prefix (CP) in guard interval, parallel/serial (P/S), digital-to-analog converter (DAC) and radio frequency to optical up-converter (RTO) are necessary elements as given in Fig.3. On the other hand, before OFDM demodulation in the downlink receiver, the corresponding offline DSP functions consists of preprocessing stage, i.e., adding noise to signal, direct current (DC) blocking and normalization, and main algorithm stage, i.e., Bessel filtering, re-sampling, quadrature imbalance, chromatic dispersion, nonlinear compensation, timing recovery, adaptive equalizer, down-sampling, frequency offset estimation (FOE) and carrier phase estimation (CPE), which can be successfully performed to improve the system performance, decrease the computational complexity and save cost.

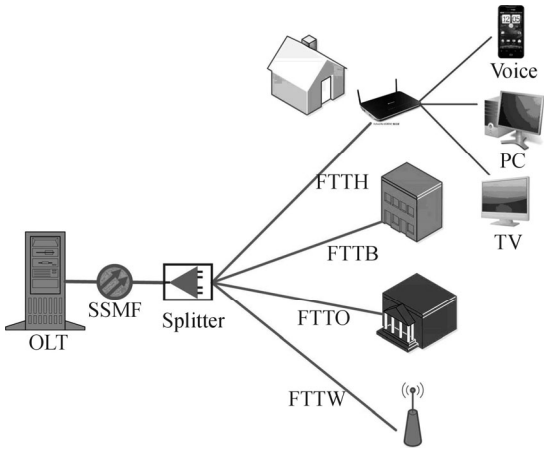

Fig.1 Schematic diagram of architecture for optical access systems

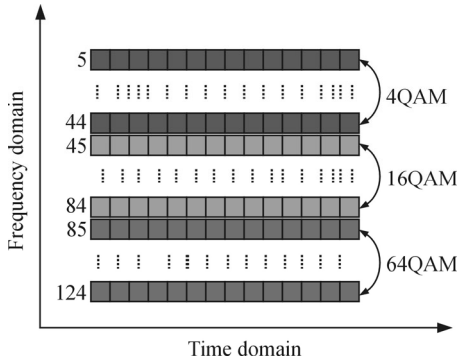

Fig.2 Subcarrier allocation of hybrid modulation scheme

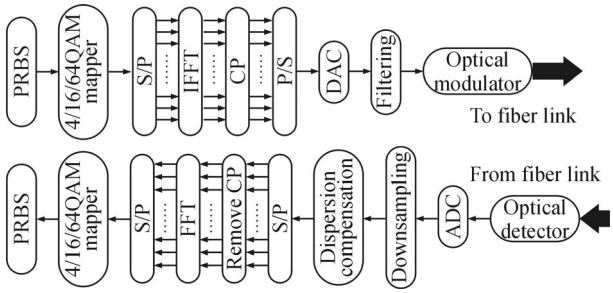

Fig.3 Schematic diagram of the proposed optical OFDM based on hybrid IFFT/FFT

Fig.4 shows the system setup for the proposed scheme with the downlink configuration adopting optical OFDM signals, which can realize up to 40 Gbit/s hybrid 4/16/64QAM-OFDM signal, and the uplink configuration based on NRZ optical signals transmitting over 20-km-long SSMF. At the OLT, the continuous wavelength (CW) light wave functioned as optical carrier signal from external cavity laser1 (ECL1) at 193.1 THz with the line width less than 0.1 MHz, the initial phase of only 0° and the output power of 10 dBm is first modulated by an 40 Gbit/s electrical binary signal in an I/Q modulator used for optical up-conversion. One cross coupler with coupling coefficient of 0.5 is used to split optical signal into two branches, two parallel LiNb Mach-Zehnder modulators (MZMs) with bias voltage of 4 V is used to realize electrical-to-optical conversion (EOC) and generate the intensity modulated optical OFDM signal, a phase shifter (PS) is used to add a time phase delay of 90° to one of the optical input signal, and another cross coupler is used to recombine the two optical signal transmitted over two branches into one branch. Then an optical coupler (OC) with coupling coefficient of 0.5 and additional loss less than 0 dB is used to combine both the modulated optical signal and another optical carrier signal from ECL2 at 193.2 THz whose operating wavelength is different from that of ECL1. Finally the mixing signal is promoted by erbium doped fiber amplifier (EDFA1) with the gain of 5 dB and the noise figure of 4 dB, in order to generate hybrid 4/16/64QAM-OFDM modulated optical baseband signal. Subsequently, the generated 4/16/64QAM OFDM modulated optical baseband signal is directly sent into the 20-km-long SSMF-28 at 1 550 nm reference wavelength with the launched optical power (*LOP*) of 15 dBm, the optical attenuation of 0.2 dB/km, the CD coefficient of 16.75 ps/(nm·km) and the polarization mode dispersion (PMD) coefficient fixed at 0.05 ps/km$^{1/2}$, without the help of the optical dispersion compensation.

At the ONU, the received hybrid 64/16/4QAM OFDM optical signal is first injected into an passive optical splitter (OS) to separate the input signal into two output signals. One is used for coherent detection at downlink receiver after Bessel optical bandpass filter (BPF1) with the center frequency of 193.1 THz, 3-dB bandwidth of 10 GHz and modulation order of 3 level. Another is applied for uplink transmitter after Bessel optical BPF2 with a center frequency of 193.2 THz and a 3-dB bandwidth of 10 GHz, then attenuated by variable optical attenuator (VOA) with power attenuation factor varying from 0 to 30 dB to bridge the gap between transmitter end and receiver end in the form of optical signal-to-noise ratio (*OSNR*), and finally detected by the CW light wave from ECL3 functioned as local oscillator (LO) with operating wavelength the same as that of the received optical signal in 90° optical hybrid composed of four 3-dB optical couplers and a PS. Furthermore, four parallel output optical signals are directly detected by 4 PIN photodiodes with the responsivity of 1 A/W, the 3-dB bandwidth of 10 GHz and the sample rate of 4×10^{10} s^{-1} to convert the optical signal into electrical signal. After that, each two electrical signals are dealt by electrical subtractor to form in-phase and quadrature signal. Next, to the best of our knowledge, offline DSP is of great importance in OFDM demodulation.

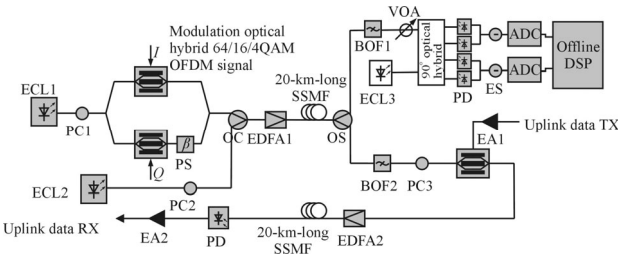

Fig.4 System setup of the proposed scheme with downlink and uplink

At the ONU, the bit sequence generated by pseudo-random bit sequence (PRBS) generator according to different operation modes is first coded by NRZ pulse generator to produce electrical signal, and then modulated by the second optical carrier signal after the BPF2 with center frequency of 193.2 THz coming from the receiver of downlink transmission in MZM, which has extinction ratio of 30 dB and symmetry factor of −1. After this, the non-chirped baseband signal is sent into 20-km-long SSMF (SMF-28) with the *LOP* of 10 dBm, which has features identical to that of the optical fiber for downlink transmission. As such, at the OLT side for uplink transmission, in order to adjust the *ROP* to meet the *LOP*, namely, *OSNR* measurement, an EDFA2 is employed to pre-amplify the received optical signal before a PIN photodiode with responsivity of 1 A/W and sample rate of 4×10^{10} s^{-1}. There is a low pass Bessel filter with a cutoff frequency of 0.75×symbol rate between the PIN photodiode and the retiming, reshaping and reamplifying (3R) regenerator to filter redundancy noise and get net signal. The key parameters of the OFDM-PON system for downlink part are summarized in Tab.1.

Fig.5(a) shows the optical spectrum before optical combiner at the OLT with an optical OFDM bandwidth of 9 GHz, and there is power difference between the main-lobe and the side-lobe. Fig.5(b) illustrates the optical spectrum after optical combiner at the OLT, and the frequency interval and power difference of the modulated optical 4/16/64QAM OFDM baseband signal and the local oscillator (LO) functioned as optical carrier signal are 100 GHz and 22.4 dBm, respectively. The optical spectrum after optical splitter at the ONU is given in Fig.5(c), and due to noise and dispersion transmitted over the fiber link, the two signals are successfully connected. Fig.5(d) describes the optical spectrum at center frequency of 193.1 THz after the optical BPF1. Meanwhile, the optical spectrum after the optical BPF2 is pre-

sented in Fig.5(e), which is from ECL2 entirely.

Tab.1 Key parameters of the proposed OFDM-PON system

Items	Values
Bit rate	40 Gbit/s
Symbol rate	10^{10} s^{-1}
Sequence length	32 768 bit
IFFT/FFT	128
Used subcarrier	120
Types of cyclic prefix	Symbol extension
Number of prefix points	32
Subcarrier locations	5—44; 45—84; 85—124
Modulation formats per port	4QAM; 16QAM; 64QAM
DAC sample rate	40 Gbit/s
Number of training symbols	10
Pilot symbols	5;24;44;45;64;84; 85;94;104;114;124
Fiber length	20 km

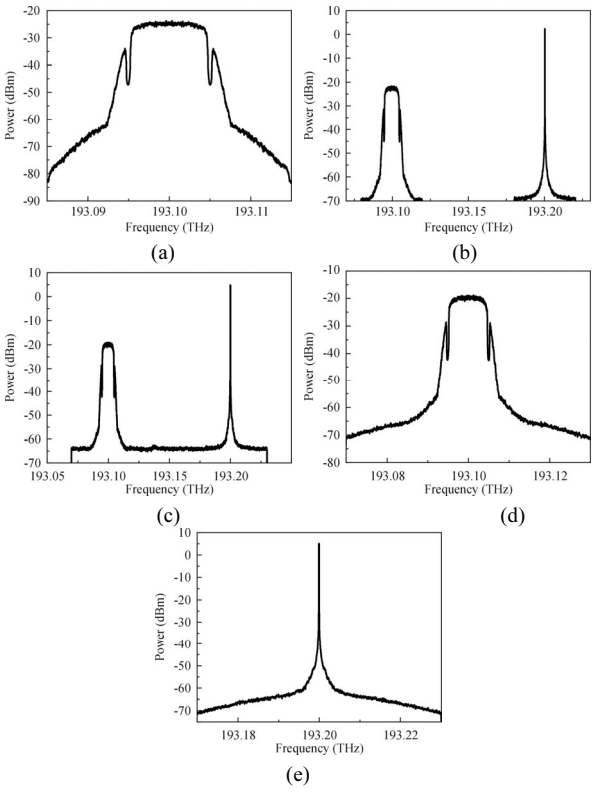

Fig.5 Optical spectra for downlink (a) before OC, (b) after OC, (c) after OS, (d) after BPF1 and (e) after BPF2

Fig.6 depicts the system performance in the form of the bit error ratio (*BER*) versus the *ROP* for 40 Gbit/s hybrid 4/16/64QAM OFDM optical signal for downlink transmitting over the 20-km-long SSMF. The *ROP* is measured at the input end of the coherent optical receiver enabled by VOA. We can see that the curve of 64QAM-OFDM first reaches the FEC limitation at the *ROP* of −13.5 dBm, then that of 16QAM-OFDM reaches at the *ROP* of −24.5 dBm, finally that of 4QAM-OFDM reaches at the *ROP* of −34 dBm. In order to keep normal communication, it can be concluded from Fig.6 that the *ROP* must be controlled in the range from −10 dBm to −15 dBm. This indicates that the transmission performance of hybrid 64/16/4QAM OFDM signal is easily influenced by the *ROP*. It can be clearly seen that the *BER* of the downlink hybrid data after 20-km-long SMF-28 transmission linearly decreases from −2.0 to −3.8 by enhancing the *ROP* from −40 dBm to −10 dBm. Compared with the single port M-QAM OFDM system, low level QAM maintains the same performance as that of hybrid modulation formats locating the corresponding subcarriers. On the other hand, the high level M-QAM OFDM signal keeps better performance under the FEC limitation. On the contrary, the performance is much worse than the hybrid modulation over the receiver sensitivity. And then, the reason is that high level M-QAM OFDM optical signals are most easily influenced by *OSNR* degradation. As can be seen from Fig.6, hybrid 64/16/4QAM OFDM formats applying for PON can reach the communicational requirements compared with the traditional modulation pattern.

Fig.7 shows the constellation diagrams for hybrid 4QAM/16QAM/64QAM transmission. Figs.6(a), (d) and (g) present constellation diagrams before channel estimation based on 10 training OFDM symbols for 4/16/64QAM OFDM, respectively. The constellation diagrams after channel estimation for 4/16/64QAM OFDM are depicted in Figs.6(b), (e) and (h), respectively. In addition, Figs.6(c), (f) and (i) demonstrate the constellation diagrams after carrier phase estimation based on pilot symbols located in Tab.1, respectively. At the same time, the constellation diagrams for 4/16/64QAM OFDM signals are experimentally measured at the *ROP* of −34.118 dBm, −24.114 dBm and −11.878 dBm, namely, the corresponding $\log_{10}BER$ are −3.05, −3.18 and −3.19, respectively.

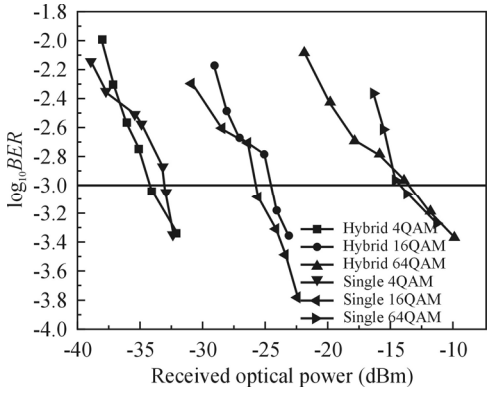

Fig.6 *BER* performance versus *ROP* for downlink over 20-km-long SSMF

Fig.8(a) and (b) illustrate the eye diagrams of transmitter and receiver used for the uplink part based on NRZ signal transmission over 20-km-long SSMF, respectively,

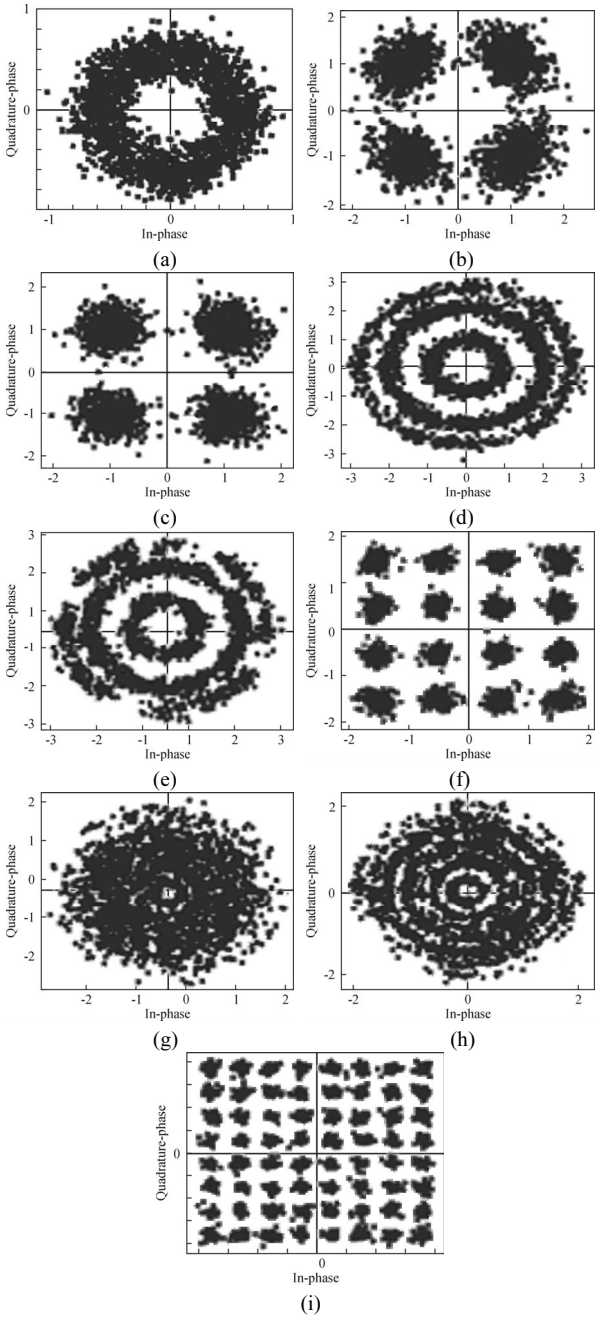

Fig.7 Constellation diagrams of (a)-(c) 4QAM, (d)-(f) 16QAM, (g)-(i) 64QAM based on hybrid IFFT/FFT

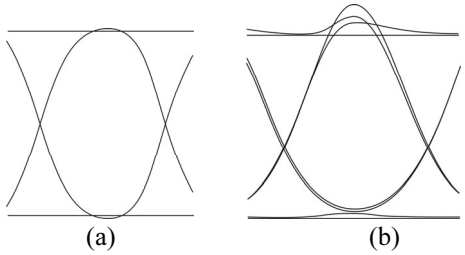

Fig.8 Eye diagrams of NRZ uplink for (a) transmitting terminal and (b) receiving terminal

in which the optimum sampling moment is 0.5 bit period, and the hypotenuse slope based on eye diagram is more sensitive to system jitter. The difference between the transmitter and the receiver exists due to amplifier spontaneous emission (ASE) noise.

We design and demonstrate in simulation a simple full-duplex PON system that consists of both 40 Gbit/s hybrid 4/16/64-QAM OFDM signal enabled by advanced DSP used for downlink transmission part and 10 Gbit/s NRZ modulation signal applied to uplink transmission part. The results show that the proposed method is regarded as more practical in the limited bandwidth resource. After 20-km-long SSMF transmission, the *BER* less than HD-FEC limitation for 4QAM, 16QAM and 64QAM OFDM link can be successfully acquired in the proposed system.

References

[1] Deng M L, Cao B Y, Giddings R P, Dong Y X, Jiang N, Nesset D, Qiu K and Tang J M, IEEE Photonics Journal **7**, 7200112 (2015).

[2] Yuan Jian-guo, Li Zhang-chao, Hu Yun-xia, Sheng Quan-liang, Lin Jin-zhao and Pang Yu, Journal of Optoelectronics·Laser **26**, 75 (2015). (in Chinese)

[3] Giacoumidis E, Kavatzikidis A, Tsokanos A, Tang J M and Tomkos I, IEEE Journal of Optical Communication and Networking **4**, 769 (2012).

[4] Halabi F, Chen L, Parre S, Barthomeuf S, Giddings R P Aupetit-Berthelemot C, Hamié A and Tang J M, Journal of Lightwave Technology **34**, 2228 (2016).

[5] Zhang S, Bai S, Bai C, Luo Q and Fang W, Optoelectronics Letters **10**, 140 (2014).

[6] Zhou Z, Bi M, Xiao S, Zhang Y and Hu W, IEEE Photonics Technology Letters **27**, 470 (2015).

[7] Bertignono L, Ferrero V, Valvo M and Gaudino R, Journal of Lightwave Technology **34**, 2064 (2016).

[8] Cano I N, Lerin A and Prat J, IEEE Photonics Technology Letters **28**, 35 (2016).

[9] Mu H, Wang M and Jian S, Optoelectronics Letters **10**, 455 (2014).

[10] Sales V, Segarra J, Polo V and Part J, IEEE Photonics Technology Letters **27**, 257 (2015).

[11] Zhang W, Zhang C, Jin W, Chen C, Jiang N and Qiu K, IEEE Photonics Technology Letters **26**, 1964 (2014).

[12] Hu X, Yang X, Shen Z, He H, Hu W and Bai C, IEEE Photonics Technology Letters **27**, 2429 (2015).

[13] Lefebvre K, Nguyen A T and Rusch L A, Journal of Lightwave Technology **32**, 3854 (2014).

[14] Zhang W, Zhang C, Chen C, Jin W and Qiu K, IEEE Photonics Technology Letters **28**, 998 (2016).

[15] Chen M, Xiao X, Yu J, Li F, Huang Z R and Zhou H, IEEE Photonics Journal **8**, 1 (2016).